



**FAU**

FRIEDRICH-ALEXANDER-  
UNIVERSITÄT  
ERLANGEN-NÜRNBERG  
SCHOOL OF ENGINEERING

# Compressed Sensing Magnetic Resonance Imaging

A. Maier, **E. Hoppe**, M. Schneider, F. Lugauer, J. Wetzl

Pattern Recognition Lab, Friedrich-Alexander-Universität Erlangen-Nürnberg

September 22, 2020



## Outline

**The Mathematics of Compressive Sampling [1,2]**

**Compressed Sensing for MRI [3]**

**Compressed Sensing Applications**

3-D Cartesian, Abdominal T1 Mapping [4]

CINE Imaging [5]



**FAU**

FRIEDRICH-ALEXANDER-  
UNIVERSITÄT  
ERLANGEN-NÜRNBERG  
SCHOOL OF ENGINEERING

# The Mathematics of Compressive Sampling [1,2]



## Nyquist/Shannon sampling theory

- The **bandwidth of a signal** determines the number of samples needed: To reconstruct a signal without error, the sampling rate has to be (at least) **twice the maximum signal frequency**.

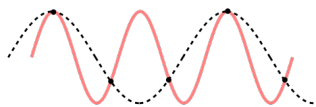


Figure: The sine wave with the higher frequency violates the Nyquist/Shannon sampling theorem  
(Source: <https://en.wikipedia.org/wiki>).

## Nyquist/Shannon sampling theory

- The **bandwidth of a signal** determines the number of samples needed: To reconstruct a signal without error, the sampling rate has to be (at least) **twice the maximum signal frequency**.
- If the signal is not bandlimited, the required **spatial/temporal resolution** determines the required sampling rate

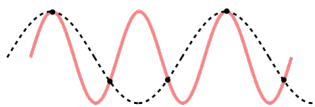


Figure: The sine wave with the higher frequency violates the Nyquist/Shannon sampling theorem  
(Source: <https://en.wikipedia.org/wiki>).

## Nyquist/Shannon sampling theory

- The **bandwidth of a signal** determines the number of samples needed: To reconstruct a signal without error, the sampling rate has to be (at least) **twice the maximum signal frequency**.
- If the signal is not bandlimited, the required **spatial/temporal resolution** determines the required sampling rate
- If an image is for example sampled in the Fourier domain, the acquired samples have to (at least) match the desired image resolution

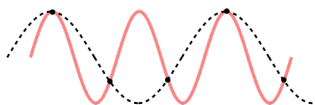


Figure: The sine wave with the higher frequency violates the Nyquist/Shannon sampling theorem  
(Source: <https://en.wikipedia.org/wiki>).

## Sparsity

- However, in some cases the number of required measurements/samples is far smaller than stated in the conventional sampling theorem → **sparse representation in a certain domain**

## Sparsity

- However, in some cases the number of required measurements/samples is far smaller than stated in the conventional sampling theorem → **sparse representation in a certain domain**
- A vector  $\mathbf{x} \in \mathbb{R}^N$  is **S-sparse**, if its support  $\{i : x_i \neq 0\}$  is of cardinality less or equal to  $S$

## Sparsity

- However, in some cases the number of required measurements/samples is far smaller than stated in the conventional sampling theorem → **sparse representation in a certain domain**
- A vector  $\mathbf{x} \in \mathbb{R}^N$  is **S-sparse**, if its support  $\{i : x_i \neq 0\}$  is of cardinality less or equal to  $S$
- The vector  $\mathbf{x}$  might be the vertical concatenation of an image, or may contain coefficients of a signal

$$f(t) = \sum_{i=1}^N x_i \psi_i(t), \quad t = 1, \dots, N,$$

which was expanded based on an **orthonormal basis**  $\psi_i(t)$ .

# Sparsity

- In matrix notation:

$$\mathbf{x} = \Psi \mathbf{f}, \quad \mathbf{f} = \Psi^* \mathbf{x},$$

where  $\Psi = [\psi_1, \dots, \psi_N]^T \in \mathbb{R}^{N \times N}$  is called **sparsity basis** or **sparsity transform**.

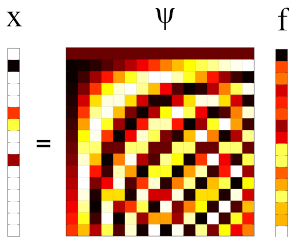


Figure: Exemplary decomposition of a signal  $\mathbf{f}$  into its sparse representation  $\mathbf{x}$  using discrete cosine transform (DCT).

# Sparsity

- The signal is then called to be sparse in the  $\Psi$ -domain

# Sparsity

- The signal is then called to be sparse in the  $\Psi$ -domain
- The sparsity transform can for instance be formed by **wavelets, B-splines, DCT, sinusoids, Dirac delta functions**, etc.

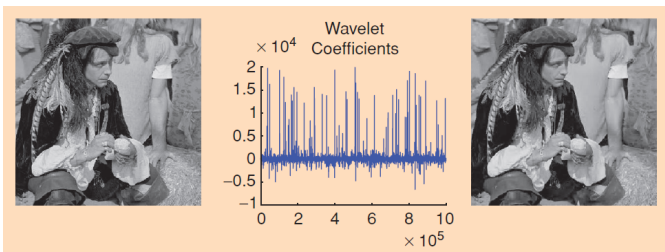


Figure: Original greyscale image (left), its arbitrarily ordered wavelet coefficients (middle), and the compressed reconstruction (right) that makes use of the 25000 largest wavelet coefficients (Source: [2]).

## Undersampled measurements

- The signal  $f(t)$  is correlated and sampled with the **sensing waveforms**  $\phi_k(t)$ ,  $k = 1, \dots, K$  using the **linear measurements**  $y_k = \langle \mathbf{f}, \phi_k \rangle$ .

## Undersampled measurements

- The signal  $f(t)$  is correlated and sampled with the **sensing waveforms**  $\phi_k(t)$ ,  $k = 1, \dots, K$  using the **linear measurements**  $y_k = \langle \mathbf{f}, \phi_k \rangle$ .
- The waveforms  $\phi_k(t)$  are for example spikes, indicator functions of pixels or sinusoids, etc.

## Undersampled measurements

- The signal  $f(t)$  is correlated and sampled with the **sensing waveforms**  $\phi_k(t)$ ,  $k = 1, \dots, K$  using the **linear measurements**  $y_k = \langle \mathbf{f}, \phi_k \rangle$ .
- The waveforms  $\phi_k(t)$  are for example spikes, indicator functions of pixels or sinusoids, etc.
- In **compressed sensing** the **underdetermined** case is of interest ( $K \ll N$ )

## Undersampled measurements

- The signal  $f(t)$  is correlated and sampled with the **sensing waveforms**  $\phi_k(t)$ ,  $k = 1, \dots, K$  using the **linear measurements**  $y_k = \langle \mathbf{f}, \phi_k \rangle$ .
- The waveforms  $\phi_k(t)$  are for example spikes, indicator functions of pixels or sinusoids, etc.
- In **compressed sensing** the **underdetermined** case is of interest ( $K \ll N$ )

### Example: Sensing frequency coefficients

Measuring undersampled data

$$y_k = \frac{1}{\sqrt{N}} \sum_{t=0}^{N-1} x_t e^{-i2\pi\omega_k t / N}$$

at frequencies  $\omega_k$ ,  $k = 1, \dots, K$  in the Fourier domain of a signal  $\mathbf{x} \in \mathbb{R}^N$ .

## Undersampled measurements

- In matrix notation:

$$\mathbf{y} = \Phi \mathbf{f} = \Phi \Psi^* \mathbf{x},$$

where  $\Phi$  is the K by N dimensional **sensing matrix**.

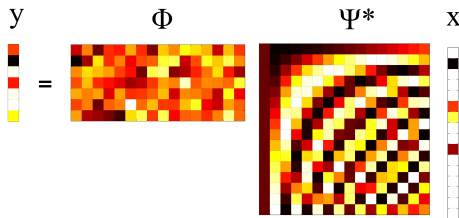


Figure: Exemplary CS measurement visualization using random sensing matrix  $\Phi$ , DCT sparsity transform and sparse coefficient vector  $\mathbf{x}$ .

## Incoherent measurements

- Measuring an object involves transforming it from the  $\Psi$  to the  $\Phi$  domain by means of the measurement and sparsity basis via the matrix  $\mathbf{U} := \Phi\Psi^*$

## Incoherent measurements

- Measuring an object involves transforming it from the  $\Psi$  to the  $\Phi$  domain by means of the measurement and sparsity basis via the matrix  $\mathbf{U} := \Phi\Psi^*$
- The transform  $\mathbf{U}$  defines the **coherence of the sampling process**, which is given by the largest correlation of any combination of  $\phi_i$ ,  $i = 1, \dots, K$  and  $\psi_j$ ,  $j = 1, \dots, N$

## Incoherent measurements

- Measuring an object involves transforming it from the  $\Psi$  to the  $\Phi$  domain by means of the measurement and sparsity basis via the matrix  $\mathbf{U} := \Phi\Psi^*$
- The transform  $\mathbf{U}$  defines the **coherence of the sampling process**, which is given by the largest correlation of any combination of  $\phi_i$ ,  $i = 1, \dots, K$  and  $\psi_j$ ,  $j = 1, \dots, N$

### Definition: Mutual coherence [1]

The mutual coherence between sensing matrix  $\Phi$  and sparsity basis  $\Psi$  is defined as

$$\mu := \sqrt{N} \max_{i,j} |\mathbf{U}_{i,j}| = \sqrt{N} \max_{i,j} |\langle \phi_i, \psi_j \rangle|$$

## Incoherent measurements

- Measuring an object involves transforming it from the  $\Psi$  to the  $\Phi$  domain by means of the measurement and sparsity basis via the matrix  $\mathbf{U} := \Phi\Psi^*$
- The transform  $\mathbf{U}$  defines the **coherence of the sampling process**, which is given by the largest correlation of any combination of  $\phi_i$ ,  $i = 1, \dots, K$  and  $\psi_j$ ,  $j = 1, \dots, N$

### Definition: Mutual coherence [1]

The mutual coherence between sensing matrix  $\Phi$  and sparsity basis  $\Psi$  is defined as

$$\mu := \sqrt{N} \max_{i,j} |\mathbf{U}_{i,j}| = \sqrt{N} \max_{i,j} |\langle \phi_i, \psi_j \rangle|$$

- The **larger the incoherence of  $(\Psi, \Phi)$ , the smaller the required samples** to accurately reconstruct the image of interest

## Norms

- $l_p$ -norm of a vector  $\mathbf{x}$  is defined as:

$$\|\mathbf{x}\|_p = \sqrt[p]{\sum_i |\mathbf{x}_i|^p}, \text{ where } p \in \mathbb{R}$$

## Norms

- $l_p$ -norm of a vector  $\mathbf{x}$  is defined as:

$$\|\mathbf{x}\|_p = \sqrt[p]{\sum_i |\mathbf{x}_i|^p}, \text{ where } p \in \mathbb{R}$$

- $l_0$ -norm:

$$\|\mathbf{x}\|_0 = \sqrt[0]{\sum_i |\mathbf{x}_i|^0}$$

## Norms

- $\ell_p$ -norm of a vector  $\mathbf{x}$  is defined as:

$$\|\mathbf{x}\|_p = \sqrt[p]{\sum_i |\mathbf{x}_i|^p}, \text{ where } p \in \mathbb{R}$$

- $\ell_0$ -norm:

$$\|\mathbf{x}\|_0 = \sqrt[0]{\sum_i |\mathbf{x}_i|^0}$$

- $\ell_1$ -norm:

$$\|\mathbf{x}\|_1 = \sum_i |\mathbf{x}_i|$$

## Norms

- $l_p$ -norm of a vector  $\mathbf{x}$  is defined as:

$$\|\mathbf{x}\|_p = \sqrt[p]{\sum_i |\mathbf{x}_i|^p}, \text{ where } p \in \mathbb{R}$$

- $l_0$ -norm:

$$\|\mathbf{x}\|_0 = \sqrt[0]{\sum_i |\mathbf{x}_i|^0}$$

- $l_1$ -norm:

$$\|\mathbf{x}\|_1 = \sum_i |\mathbf{x}_i|$$

- $l_2$ -norm:

$$\|\mathbf{x}\|_2 = \sqrt{\sum_i |\mathbf{x}_i|^2}$$

## Non-linear sampling theorem

- To estimate  $\mathbf{f} \in \mathbb{R}^N$  from undersampled measurements  $\mathbf{y} \in \mathbb{R}^K$  we have to find the decomposition of  $\mathbf{f}$  with minimum  $l_1$ -norm that is consistent with the measurements.

## Non-linear sampling theorem

- To estimate  $\mathbf{f} \in \mathbb{R}^N$  from undersampled measurements  $\mathbf{y} \in \mathbb{R}^K$  we have to find the decomposition of  $\mathbf{f}$  with minimum  $l_1$ -norm that is consistent with the measurements.
- This leads to the following nonlinear reconstruction problem

**Theorem: Nonlinear sampling theorem [1]**

$$\begin{aligned} & \text{Minimize}_{\tilde{\mathbf{x}} \in \mathbb{R}^N} && \|\tilde{\mathbf{x}}\|_{l_1} \\ & \text{s.t.} && \Phi \Psi^* \tilde{\mathbf{x}} = \mathbf{y}. \end{aligned}$$

## Robust compressive sampling

- Any measurement of a sensor in a real application is subject to a superimposed **noise component**  $\rightarrow \mathbf{y} = \Phi\mathbf{f} + \mathbf{e}$ , where the noise term has limited energy:  $\|\mathbf{e}\|_2 \leq \epsilon$ .

## Robust compressive sampling

- Any measurement of a sensor in a real application is subject to a superimposed **noise component**  $\rightarrow \mathbf{y} = \Phi\mathbf{f} + \mathbf{e}$ , where the noise term has limited energy:  $\|\mathbf{e}\|_2 \leq \epsilon$ .
- The robustness with respect to noise is an important aspect of every compressed sensing algorithm

## Robust compressive sampling

- Any measurement of a sensor in a real application is subject to a superimposed **noise component**  $\rightarrow \mathbf{y} = \Phi\mathbf{f} + \mathbf{e}$ , where the noise term has limited energy:  $\|\mathbf{e}\|_2 \leq \epsilon$ .
- The robustness with respect to noise is an important aspect of every compressed sensing algorithm
- The following minimization problem takes **stochastic** or **deterministic** inaccuracies in the observed data into account:

**Theorem: Noise-aware, nonlinear sampling theorem [1]**

$$\begin{aligned} \text{Minimize}_{\tilde{\mathbf{x}} \in \mathbb{R}^N} \quad & \|\tilde{\mathbf{x}}\|_1 \\ \text{s.t.} \quad & \|\Phi\Psi^*\tilde{\mathbf{x}} - \mathbf{y}\|_2 \leq \epsilon. \end{aligned}$$



**FAU**

FRIEDRICH-ALEXANDER-  
UNIVERSITÄT  
ERLANGEN-NÜRNBERG  
SCHOOL OF ENGINEERING

# Compressed Sensing for MRI [3]



# Linking Compressed Sensing and MRI

## Why Compressed Sensing for MRI?

- Medical images are naturally compressible by sparse coding in an appropriate transform domain.

# Linking Compressed Sensing and MRI

## Why Compressed Sensing for MRI?

- Medical images are naturally compressible by sparse coding in an appropriate transform domain.
- MRI scanners naturally acquire encoded samples, rather than pixel samples (→ spatial-frequency encoding).

# Linking Compressed Sensing and MRI

## Why Compressed Sensing for MRI?

- Medical images are naturally compressible by sparse coding in an appropriate transform domain.
- MRI scanners naturally acquire encoded samples, rather than pixel samples ( $\rightarrow$  spatial-frequency encoding).
- We can choose the sampling trajectory to increase the incoherence.

## Compressed Sensing for MRI

- Sampled linear combinations = Fourier coefficients ( $k$ -space samples)
- Small subset of entire  $k$ -space → **Undersampling**

## Compressed Sensing for MRI

- Sampled linear combinations = Fourier coefficients ( $k$ -space samples)
- Small subset of entire  $k$ -space → **Undersampling**
- Requirements:

## Compressed Sensing for MRI

- Sampled linear combinations = Fourier coefficients ( $k$ -space samples)
- Small subset of entire  $k$ -space → **Undersampling**
- Requirements:
  - Transform **sparsity**

# Compressed Sensing for MRI

- Sampled linear combinations = Fourier coefficients ( $k$ -space samples)
- Small subset of entire  $k$ -space → **Undersampling**
- Requirements:
  - Transform **sparsity**
  - **Incoherence** of undersampling artifacts

## Compressed Sensing for MRI

- Sampled linear combinations = Fourier coefficients ( $k$ -space samples)
- Small subset of entire  $k$ -space → **Undersampling**
- Requirements:
  - Transform **sparsity**
  - **Incoherence** of undersampling artifacts
  - **Non-linear** reconstruction

# Compressed Sensing for MRI: Requirements

## Transform sparsity

- Most MR images are sparse in an appropriate **transform domain**
- Examples:
  - Angiograms → already pixel domain (or e.g. finite-differences)
  - Brain → wavelet domain
  - Quasi-periodicity of heart images → sparse temporal Fourier transform

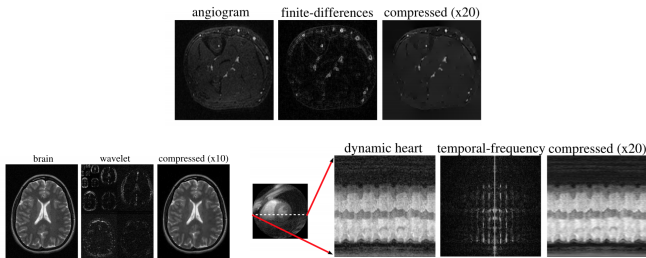


Figure: Different MR images and their sparse transform domains (Source [3]).

# Compressed Sensing for MR: Requirements

## Incoherence of undersampling artifacts

- Example:
  - Sparse signal (1), sub-Nyquist (8-fold) sampled in its  $k$ -space (2)
  - Zero-filling the missing values
  - Equispaced (2, bottom) vs. random (2, top) undersampling

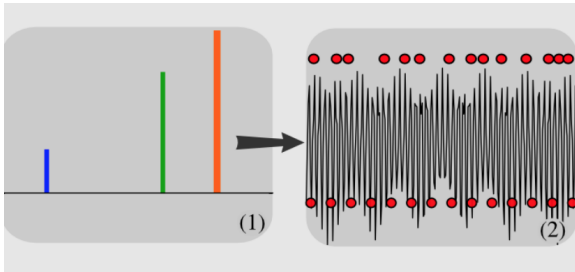


Figure: 1-D sparse signal and its undersampling in  $k$ -space (Source: [3]).

# Compressed Sensing for MR: Requirements

## Incoherence of undersampling artifacts

- **Equispaced undersampling (3a)**  
→ Artifacts depending on sampling pattern
- **Random undersampling (3)**  
→ Incoherent artifacts behave much like additive random noise

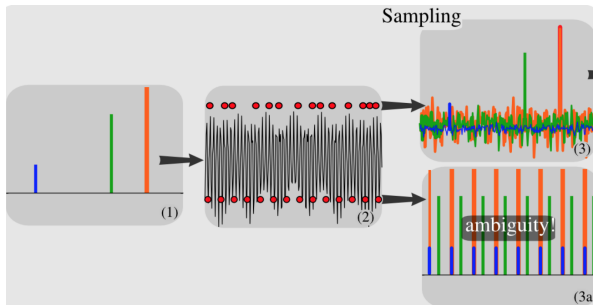


Figure: Different undersamplings (Source: [3]).

# Compressed Sensing for MR: Requirements

## Incoherence of undersampling artifacts

- Iterative reconstruction:
  - Iterative thresholding (4)
  - Pick largest components (5)
  - Calculate the interference caused by them (6)
  - Subtract it (7)
  - Repeat with smaller components

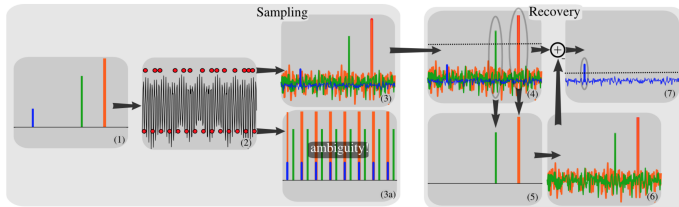


Figure: Iterative reconstruction (Source: [3]).

# Incoherent Sampling for MRI

## Compressed Sensing scheme:

- Selection of a subset of frequency domain

# Incoherent Sampling for MRI

## Compressed Sensing scheme:

- Selection of a subset of frequency domain
- For efficient sampling

# Incoherent Sampling for MRI

## Compressed Sensing scheme:

- Selection of a subset of frequency domain
- For efficient sampling
- Which is incoherent with respect to the sparsifying transform

## Incoherence: Quantitative

Transform Point Spread Function (TPSF):

$$TPSF(i, j) = (\Psi^* \mathcal{F}_S^* \mathcal{F}_S \Psi)(i, j)$$

$\Psi$ : Sparsifying transform

$\Psi^*$ : Adjoint operation of  $\Psi$

$\mathcal{F}_S$ : Fourier transform at frequencies in subset  $S$

$\mathcal{F}_S^*$ : Adjoint operation (zero-filling and inverse Fourier transform)

## Incoherence: Quantitative

Transform Point Spread Function (TPSF):

$$TPSF(i, j) = (\Psi^* \mathcal{F}_S^* \mathcal{F}_S \Psi)(i, j)$$

$\Psi$ : Sparsifying transform

$\Psi^*$ : Adjoint operation of  $\Psi$

$\mathcal{F}_S$ : Fourier transform at frequencies in subset  $S$

$\mathcal{F}_S^*$ : Adjoint operation (zero-filling and inverse Fourier transform)

→ Coherence formally measured by  $\max_{i \neq j} \|TPSF(i, j)\|$

## Incoherent Sampling: Trajectories

- Truly random subset of  $k$ -space: impractical

## Incoherent Sampling: Trajectories

- Truly random subset of  $k$ -space: impractical
- Most energy concentrated in the center of  $k$ -space → **variable-density sampling**

## Incoherent Sampling: Trajectories

- Truly random subset of  $k$ -space: impractical
- Most energy concentrated in the center of  $k$ -space → **variable-density sampling**
- Irregular trajectories → mimic **coincidence** and allow **rapid sampling**

# Incoherent Sampling: Trajectories

Different trajectories:

- Cartesian sampling
- Radial sampling
- Spiral sampling
- Dynamic images

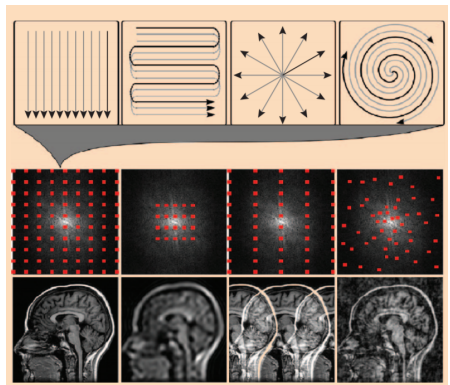
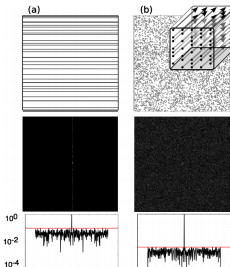


Figure: Different trajectories and undersampling artifacts in linear reconstructions (Source: [3]).

# Incoherent Sampling: Trajectories

## Cartesian sampling

- Parallel equispaced lines →  $n_{pe} \times n_{fe}$  samples (for 3-D:  $n_{pe} \times n_{se} \times n_{fe}$ )  
 $n_{pe}$ : Phase encodes  $n_{fe}$ : Frequency encodes  $n_{se}$ : Slice encodes
- Skip certain acquisitions → Undersampled parallel lines



## Coherence:

- 2-D: one undersampled dimension → 1-D sparsity
- (a)
- 3-D: two undersampled dimensions → 2-D cross-sections (b)

Figure: TPSFs of Cartesian sampling. Random lines in 2-D (a), random points in 2-D/cross-section of random lines in 3-D. Bottom: Lineplot of TPSF, height of red lines measures coherence (Source: [3]).

# Incoherent Sampling: Trajectories

## Radial and variable-density spiral sampling

- Benign artifacts → incoherent TPSF
- Can be suppressed with appropriate non-linear reconstruction without degrading image quality

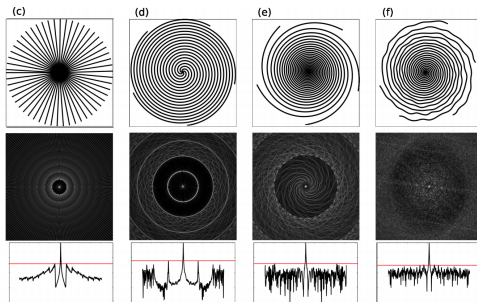


Figure: TPSFs of radial sampling (c), uniform spirals (d), variable density spirals (e) and variable density perturbed spirals (f). Bottom: Lineplot of TPSF, height of red lines measures coherence (Source: [3]).

# Incoherent Sampling: Trajectories

## Dynamic images

- Spatial coordinates + time as an additional dimension  $\rightarrow (k - t)$  domain
- Randomly ordering of the lines  $\rightarrow$  random sampling of the  $k - t$  space
- This is incoherent with respect to the spatial vs. temporal frequency  $x - f$  domain

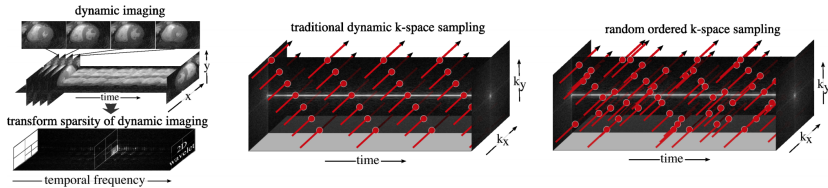


Figure: Sparsity and sampling of dynamic images (Source: [3]).

# Image Reconstruction

Constrained optimization problem:

$$\text{minimize} \quad \|\Psi m\|_1$$

$$s.t. \quad \|\mathcal{F}_S m - y\|_2 < \epsilon$$

$m$ : Reconstructed image (complex vector)

$\Psi$ : Linear operator from pixel to the chosen representation

$\mathcal{F}_S$ : (Undersampled) Fourier transform

$y$ : Measured  $k$ -space data

$\epsilon$ : Threshold parameter, expected noise level

- Minimizing  $l_1$  norm of  $\|x\|_1 = \sum_i \|x_i\| \rightarrow \text{sparsity}$
- Constraint  $\|\mathcal{F}_S m - y\|_2 < \epsilon \rightarrow \text{data consistency}$

# Non-linear, Iterative Reconstruction: Summary

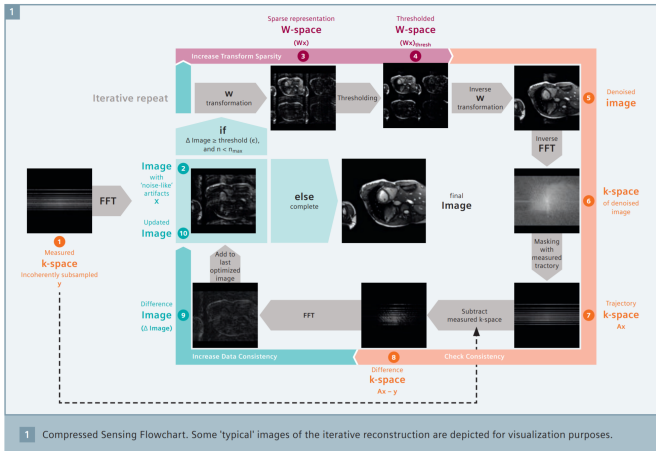


Figure: Summary of the compressed sensing-based, non-linear, iterative reconstruction process (Source: [https://mriquestions.com/uploads/3/4/5/7/34572113/siemens\\_mri\\_magnetom-world\\_compressed-sensing\\_compressed-sensing-flowchart\\_blaeche-03520147.pdf](https://mriquestions.com/uploads/3/4/5/7/34572113/siemens_mri_magnetom-world_compressed-sensing_compressed-sensing-flowchart_blaeche-03520147.pdf)).

# Iterative Reconstruction: Simple example

## Objective function:

$$f(x) = \frac{1}{2}|\mathbf{y} - \mathbf{P}\mathbf{F}^H\mathbf{x}|_2^2 + \lambda|\mathbf{Wx}|_1$$

**y**: k-space coefficients

**x**: Reconstructed image

**F<sup>H</sup>**: Inverse Fourier Transform

**P**: Undersampled matrix

**W**: Wavelet transform

# Iterative Reconstruction: Simple example

**Objective function:**

$$f(x) = \frac{1}{2}|\mathbf{y} - \mathbf{P}\mathbf{F}^H\mathbf{x}|_2^2 + \lambda|\mathbf{Wx}|_1$$

**y:** k-space coefficients

**x:** Reconstructed image

**F<sup>H</sup>:** Inverse Fourier Transform

**P:** Undersampled matrix

**W:** Wavelet transform

**Iterative reconstruction with wavelet shrinkage:**

# Iterative Reconstruction: Simple example

## Objective function:

$$f(x) = \frac{1}{2}|\mathbf{y} - \mathbf{P}\mathbf{F}^H\mathbf{x}|_2^2 + \lambda|\mathbf{Wx}|_1$$

$\mathbf{y}$ : k-space coefficients

$\mathbf{x}$ : Reconstructed image

$\mathbf{F}^H$ : Inverse Fourier Transform

$\mathbf{P}$ : Undersampled matrix

$\mathbf{W}$ : Wavelet transform

## Iterative reconstruction with wavelet shrinkage:

### 1. Data update:

$$\mathbf{x}_t = \mathbf{x}_{t-1} + s \cdot \mathbf{F}(\mathbf{y} - \mathbf{P}\mathbf{F}^H\mathbf{x}_{t-1}), \text{ where } s \text{ is the step size of the update}$$

# Iterative Reconstruction: Simple example

## Objective function:

$$f(x) = \frac{1}{2}|\mathbf{y} - \mathbf{P}\mathbf{F}^H\mathbf{x}|_2^2 + \lambda|\mathbf{Wx}|_1$$

**y**: k-space coefficients

**x**: Reconstructed image

**F<sup>H</sup>**: Inverse Fourier Transform

**P**: Undersampled matrix

**W**: Wavelet transform

## Iterative reconstruction with wavelet shrinkage:

### 1. Data update:

$$\mathbf{x}_t = \mathbf{x}_{t-1} + s \cdot \mathbf{F}(\mathbf{y} - \mathbf{P}\mathbf{F}^H\mathbf{x}_{t-1}), \text{ where } s \text{ is the step size of the update}$$

### 2. Wavelet shrinkage:

$$c(x, y) = \begin{cases} c(x, y) - \epsilon, & \text{if } |c(x, y)| > \epsilon \\ 0, & \text{Otherwise} \end{cases}$$



**FAU**

FRIEDRICH-ALEXANDER-  
UNIVERSITÄT  
ERLANGEN-NÜRNBERG  
SCHOOL OF ENGINEERING

# Compressed Sensing Applications



## T1 mapping

- Quantitative parameter maps of the **longitudinal relaxation  $T_1$**  in the abdomen are used to examine **liver or kidney function**, or for assessing diseases like e.g. **chronic pancreatitis**
- Look Locker T1 mapping** techniques continuously sample the relaxation curve after an **adiabatic inversion pulse**

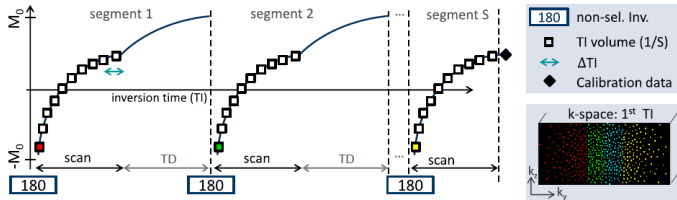


Figure: K-space is divided into several segments, and relaxations are sampled continuously

# Spatio-temporal incoherence

- The method uses a **2-D Poisson sampling scheme** with **variable density** and **spatio-temporal incoherence**

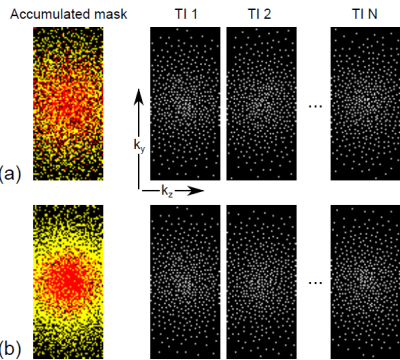


Figure: Sampling patterns for the phase encoding steps for the **accumulated masks** (left) and the **individual TI acquisitions** (right); (a) without temporal incoherence term (b) with temporal incoherence term; **red points**: sampled more than once; **yellow points**: sampled only once

# Spatio-temporal incoherence

- The method uses a **2-D Poisson sampling scheme** with **variable density** and **spatio-temporal incoherence**
- Compared to conventional **variable density Poisson sampling** (Figure (a)), additionally enforcing **temporal incoherence** (along individual TIs; Figure (b)) reduces the **number of duplicates**

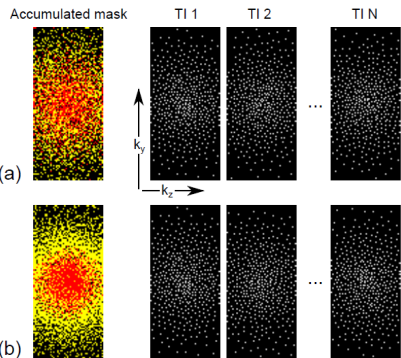


Figure: Sampling patterns for the phase encoding steps for the **accumulated masks** (left) and the **individual TI acquisitions** (right); (a) without temporal incoherence term (b) with temporal incoherence term; **red points**: sampled more than once; **yellow points**: sampled only once

# Spatio-temporal incoherence

- The method uses a **2-D Poisson sampling scheme** with **variable density** and **spatio-temporal incoherence**
- Compared to conventional **variable density Poisson sampling** (Figure (a)), additionally enforcing **temporal incoherence** (along individual TIs; Figure (b)) reduces the **number of duplicates**
- This **increases temporal incoherence**, while preserving the **Poisson properties**

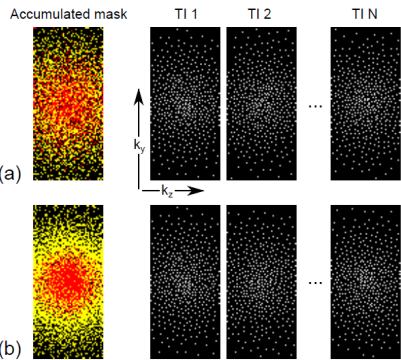


Figure: Sampling patterns for the phase encoding steps for the **accumulated masks** (left) and the **individual TI acquisitions** (right); (a) without temporal incoherence term (b) with temporal incoherence term; **red points**: sampled more than once; **yellow points**: sampled only once

## Sparsity and Iterative Reconstruction

- Reconstruction enforces spatio-temporal sparsity using single-level Haar wavelets

$$\hat{\mathbf{x}}_i = \operatorname{argmin}_{\hat{\mathbf{x}}_i} \sum_{n=1}^N \sum_{c=1}^C \frac{1}{2} \|\mathbf{U}_t \mathcal{F} \mathbf{S}_c \hat{\mathbf{x}}(n)_i - \mathbf{y}(n)_c\|_2^2 + \|\mathbf{W}_{(\sigma, \tau)} \hat{\mathbf{x}}_i\|_1, \quad i \in [1, N_x]$$

$\mathbf{x}_i \in \mathbb{C}^{N_y N_z N}$  vector of 2-D+t concatenated TI images

$\mathbf{S}_c$  coil sensitivity matrix

$\mathcal{F}$  Fourier transform

$\mathbf{U}_t$  undersampling matrix

$\mathbf{y}(n)_c$  measured data for coil  $c$  and time point  $n$

$\mathbf{W}_{(\sigma, \tau)}$  single-level Haar wavelet

$N_x, N_y, N_z$  Number of samples in x, y and z direction

$N, C$  Number of time points and coils

## Results

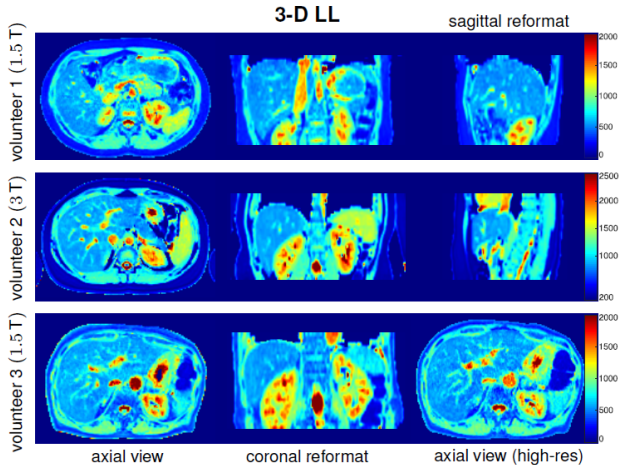


Figure: Quantitative T1 parameter maps obtained by the 3D abdominal T1 mapping method from 3 volunteers at 3T and 1.5T

# Results

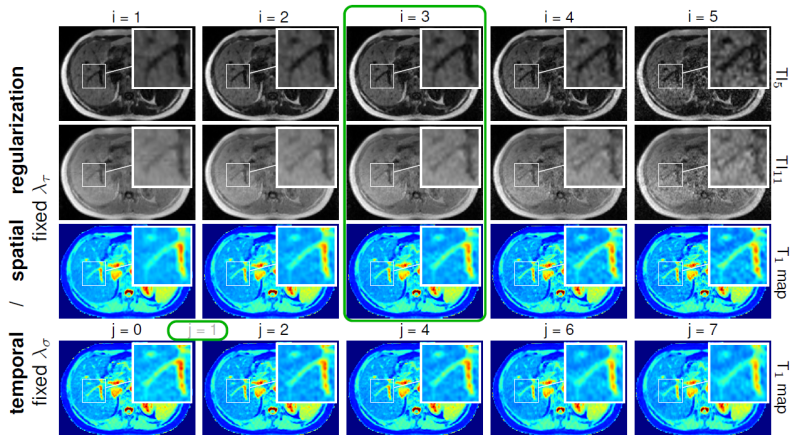


Figure: Effect of spatial (top) and temporal (bottom) regularization weights on MR images and  $T_1$  parameter maps

## 3-D MR CINE Imaging

- Images of beating heart allow diagnosis of the cardiac function

## 3-D MR CINE Imaging

- Images of beating heart allow diagnosis of the cardiac function
- Free breathing methods
  - Long acquisitions possible/needed
  - But: Data inconsistency during reconstruction

## 3-D MR CINE Imaging

- Images of beating heart allow diagnosis of the cardiac function
- Free breathing methods
  - Long acquisitions possible/needed
  - But: Data inconsistency during reconstruction
- Breath-hold methods
  - Reduce acquisition time, e.g. to single breath-hold  
→ Application of **Compressed Sensing**

## 3-D MR CINE Imaging using Cartesian Sampling

- Nearly isotropic resolution of  $1.9 \times 1.9 \times 2.5 \text{ mm}^3$  → retrospective reformatting possible
- Acquisition time fits into single breath-hold

# 3-D MR CINE Imaging using Cartesian Sampling

## Incoherent sampling pattern of the Cartesian phase-encoding plane

- Spiral phyllotaxis pattern
- Undersampled, reordered and successively rotated by a fixed angle

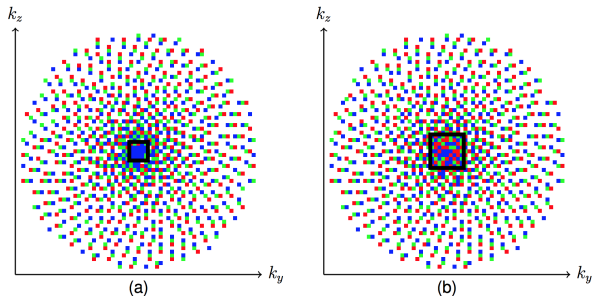


Figure: Spiral phyllotaxis pattern for 3 cardiac phases (red, green, blue).  $k$ -space center is fully sampled (outlined in black). For each  $k$ -space position with duplicates, a duplicate is randomly selected and moved to an unsampled position in its 8-neighborhood (right).

## 3-D MR CINE Imaging using Cartesian Sampling

### Incoherent sampling pattern of the Cartesian phase-encoding plane

- Spiral phyllotaxis pattern
- Undersampled, reordered and successively rotated by a fixed angle
- Extended for multiple cardiac phases with number  $T$

$$r_{n,t} = \sqrt{n/N}, \quad \varphi_{n,t} = n \cdot \pi(3 - \sqrt{5}) + t \cdot \varphi_{\text{offset}},$$

$$y_{n,t} = r_{n,t}^{v_y} \cdot \cos \varphi_{n,t}, \quad z_{n,t} = r_{n,t}^{v_z} \cdot \sin \varphi_{n,t},$$

$$v_y = v^{N_y/N_y+N_z}, \quad v_z = v^{N_z/N_y+N_z}$$

$(r_{n,t}, \varphi_{n,t})$ : Polar coordinates,  $(y_{n,t}, z_{n,t})$ : Cartesian coordinates of sample  $n$  out of  $N$  total samples for the pattern of cardiac phase  $t$

$\varphi_{\text{offset}}, v$ : empirically selected

# 3-D MR CINE Imaging using Cartesian Sampling

## Reconstruction

- Non-linear, iterative SENSitivity Encoding (SENSE) approach
- Spatio-temporal wavelet regularization

$$\begin{aligned} \{\mathbf{x}_{i,t}\}_{\substack{i \in [1,I] \\ t \in [1,T]}} &= \operatorname{argmin}_{\{\hat{\mathbf{x}}_{i,t}\}} \sum_{i=1}^I \sum_{t=1}^T \sum_{c=1}^C \|\mathbf{A}_t \mathbf{F} \mathbf{S}_{i,c} \hat{\mathbf{x}}_{i,t} - \mathbf{y}_{t,c}\|_2^2 \\ &\quad + \lambda_\omega \cdot I_{\max} \sum_{i=1}^I \sum_{t=1}^T \|\mathbf{W}_\omega \hat{\mathbf{x}}_{i,t}\|_1 + \lambda_\tau \cdot I_{\max} \sum_{i=1}^I \|\mathbf{W}_\tau (\hat{\mathbf{x}}_{i,1}^\top, \dots, \hat{\mathbf{x}}_{i,T}^\top)^\top\|_1 \end{aligned}$$

$C$ : Number of coils

$\mathbf{A}_t$ : Sampling pattern for time  $t$

$\mathcal{F}$ : Fourier transform

$\mathbf{S}_{i,c}$ : Element-wise multiplication by the  $i^{th}$  sensitivity map of coil  $c$

$\mathbf{y}_{t,c}$ : Measured data for time  $t$  and coil  $c$

$\lambda_\omega, \lambda_\tau$ : Spatial and temporal regularization parameters

$\mathbf{W}_\omega, \mathbf{W}_\tau$ : Spatial and temporal single-level redundant Haar wavelet transforms

$I_{\max}$ : Maximum image intensity for scaling the regularization parameters

# 3-D MR CINE Imaging using Cartesian Sampling

## Results

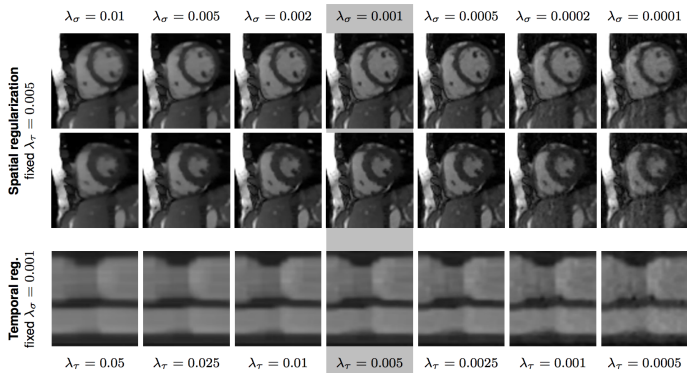


Figure: Effect of spatial and temporal regularization weights on 3-D CINE images.

**Thank you!**

## References

1. E. J. Candès et al., "Compressive sampling", in Proceedings of the international congress of mathematicians, Madrid, Spain, vol. 3, 2006, pp. 1433–1452.
2. E. J. Candès and M. B. Wakin, "An introduction to compressive sampling", IEEE signal processing magazine, vol. 25, no. 2, pp. 21–30, 2008.
3. M. Lustig, D. L. Donoho, J. M. Santos, and J. M. Pauly, "Compressed sensing mri", IEEE signal processing magazine, vol. 25, no. 2, pp. 72–82, 2008.
4. F. Lugauer et al., "Single-breath-hold abdominal T1 mapping using 3D Cartesian Look-Locker with spatiotemporal sparsity constraints". Magnetic Resonance Materials in Physics, Biology and Medicine, Vol. 31, No. 3, pp. 399–414, 2018.
5. J. Wetzl et al., "Single-breath-hold 3-d cine imaging of the left ventricle using cartesian sampling", Magnetic Resonance Materials in Physics, Biology and Medicine, pp. 1–13, 2017.